Molecular Cell, Volume *49*

Supplemental Information

A SWI/SNF Chromatin-Remodeling Complex Acts in Noncoding RNA-Mediated Transcriptional Silencing

Yongyou Zhu, M. Jordan Rowley, Gudrun Böhmdorfer, and Andrzej T. Wierzbicki

SUPPLEMENTAL EXPERIMENTAL PROCEDURES

Yeast two hybrid

The full length cDNA of IDN2 was generated by PCR and cloned into pAS2 vector (Clontech). Yeast Y190 cells containing pAS2-IDN2 plasmid were transformed with *Arabidopsis* yeast two hybrid cDNA library, (ABRC stock #CD4-22 (Kim et al., 1997)), and screened on dropout medium lacking leucine, tryptophan, and histidine but containing 50mM 3-aminotriazol. To test the interaction between two proteins in yeast, the full length cDNAs were cloned into pENTR/D-Topo vector (Invitrogen) to produce entry clones according to manufacturer's instructions. All the entry constructs were subsequently transferred to destination vector pGADT7-GW or pGBKT7-GW (Lawit et al., 2007), and the pGADT7/pGBKT7 empty vectors served as negative controls. All the pGBKT7-based constructs were transformed into yeast strain Y187, and all the pGADT7-based constructs were transformed into yeast strain Y190. Yeast mating of Y187 and Y190 was performed according to Clontech Yeast Protocols Handbook (1999).

Generation of transgenic plants

The full length cDNA or genomic DNA including promoter regions of *SWI3B* and *IDN2* were cloned into pENTR/D-Topo vector (Invitrogen) to produce entry clones according to manufacturer's instructions. The resulting entry plasmids were incubated with the destination vectors: pMDC107 (Curtis and Grossniklaus, 2003), pEarleyGate103 (Earley et al., 2006), pEarleyGate302 (Earley et al., 2006), or pZY35S302 with the Gateway LR Clonase™ II Enzyme Mix (Invitrogen) to obtain *IDN2p:IDN2-GFP* (pMDC107-*IDN2*), *IDN2p:IDN2-M8-GFP* (pMDC107-*IDN2-M8*), *SWI3Bp:SWI3B-FLAG* (pEarleyGate-*SWI3B*), *35S:SWI3B-GFP* (pEarleyGate103-*SWI3B*), *35S:IDN2-FLAG* (pZY35S302-*IDN2*), *35S:IDN2-GFP* (pEarleyGate103-*IDN2*), *35S:SWI3B-FLAG* (pZY35S302-*SWI3B*), and *35S:IDN2-M8-FLAG* (pZY35S302-*IDN2-M8*). To generate a binary vector pZY35S302 for 35S-driven expression of C-terminally FLAG-tagged proteins, the Gateway cassette, FLAG nucleotide sequence and OCS 3' were amplified from pEarleyGate302 (Earley et al., 2006) using Pfu DNA Polymerase (Agilent Technologies). Primers used for this and other PCR amplifications are shown in Table S1. After *Kpn*I and *Hind*III double digestion, the Gateway cassette was inserted into *Kpn*I and *Hind*III digested pCHF1 vector (Fankhauser et al., 1999). All constructed plasmids were introduced into the GV3101 strain of *Agrobacterium tumefaciens* and transformed into *Arabidopsis* plants by the floral dip method (Clough and Bent, 1998) or infiltrated into tobacco leaves (Voinnet et al., 2003).

Protein co-immunoprecipitation

Infiltrated tobacco leaves or 3-week-old *Arabidopsis* rosette leaves were ground into fine powder in liquid nitrogen, extracted using lysis buffer (50mM Tris-HCl pH 8.0, 150mM NaCl, 10mM EDTA, 10% glycerol, 1mM PMSF, 1% Plant Protease Inhibitor (Sigma), 0.5% Triton-X100 and centrifuged at 8000 rpm at 4˚C for 10 min. Resulting protein extracts were incubated with anti-GFP antibody (MBL 598, 1:1000 dilution) and 50µl of 50% slurry of Protein A agarose beads (Invitrogen). Beads were washed 3 times with the lysis buffer, and the bound proteins were eluted with 2x SDS buffer. Gel blots were analyzed using monoclonal anti-GFP antibody (Covance, MMS-118P), or monoclonal anti-FLAG antibody (Stratagene, 200472).

Chromatin-immunoprecipitation (ChIP)

ChIP was performed as described (Wierzbicki et al., 2008) with the following modifications: proceeding washes with Honda buffer, nuclei were washed once in 1 ml MNase reaction buffer (10 mM Tris-Cl pH 8, 15 mM NaCl, 60

mM KCl, 1 mM $CaCl_2$; centrifugation at 1900 g, 5 minutes at 4°C) and resuspended in 1 ml MNase reaction buffer. 250 µl aliquots of nuclei were incubated with 600 Kunitz units of Micrococcal Nuclease (NEB) at 37°C for 10 min, then sonicated with two 10 second long pulses (1 minute intervals) with a Fisher Scientific Sonic Dismembrator Model 100 (power setting 1). Immunoprecipitation was performed using 50 µl Dynabeads protein A (Invitrogen) and 2.5 µl anti-histone H3 antibody (ab1791, Abcam) or affinity purified anti-SWI3B antibody at 4°C over-night. After reversion of crosslinking, samples were incubated with 20 µg proteinase K (Invitrogen) at 65°C for 2 hours. Rabbit polyclonal anti-SWI3B antibody was raised against a C-terminal portion of the SWI3B protein (aa 248-469) expressed in bacteria and affinity purified. H3 ChIP-seq samples were treated similarly, but without MNase treatment and were sonicated eight times with 10 second long pulses. Library generation and Illumina sequencing were performed by the University of Michigan Sequencing Core.

RNA analysis

For RT-PCR total RNA from inflorescences was extracted using RNeasy Plant Mini kit (Qiagen), and treated with DNase I (Invitrogen). Real time RT-PCR was performed using One-Step qRT-PCR kit (Invitrogen) according to the manufacturer's instructions. Pol V-dependent transcripts were assayed in RNA digested with 1 unit of Turbo DNase (Ambion) and reverse transcribed with Superscript III reverse transcriptase (Invitrogen) using random primers (Invitrogen) followed by real time PCR. For RNA-seq total RNA was extracted from 2.5 weeks old seedlings using RNeasy Plant Mini kit (Qiagen). rRNA was depleted from 8µg total RNA using RiboMinus Plant Kit for RNA-seq (Invitrogen). Library generation and Illumina sequencing was performed by the University of Michigan Sequencing Core.

DNA methylation analysis

DNA methylation tests using methylation sensitive restriction endonucleases were performed as described (Rowley et al., 2011) and analyzed by PCR or real-time PCR.

MNase-seq

2g of 2.5-weeks old seedlings were ground to a fine powder in liquid nitrogen and resuspended in 15 ml Honda buffer (0.44 M Sucrose, 1.25 % Ficoll, 2.5 % Dextran T40, 20 mM HEPES-KOH pH 7.4, 10 mM $MgCl_2$, 0.5% Triton X-100, 5 mM DTT, 1 mM PMSF, 1 % plant protease inhibitors (Sigma)). After filtering through two layers of Miracloth, the filter was washed in 10 ml Honda buffer. This washing buffer was then filtered through two fresh layers of Miracloth and the combined filtrates were centrifuged (2500 g, 15 minutes at 4°C). The pellet was washed four times in 1 ml Honda buffer (centrifugation at 2500 g, 15 minutes at 4°C) and 1 ml MNase reaction buffer (10 mM Tris-Cl pH 8, 15 mM NaCl, 60 mM KCl, 1 mM $CaCl_2$; centrifugation at 3000 g, 5 minutes at 4°C) and finally resuspended in 660 µl MNase reaction buffer. 100 µl aliquots of nuclei were incubated with Micrococcal Nuclease (NEB) at 20°C for 10 minutes. To terminate the reaction, 10 µl STOP buffer (100 mM EDTA, 100 mM EGTA), 10 µl 10 % SDS and 40 µg proteinase K (Invitrogen) were added followed by an incubation at 60°C for one hour. DNA was extracted with phenol-chloroform-isoamyl alcohol and chloroform-isoamyl alcohol and precipitated with ethanol. The pellet was washed in 70% ethanol, resuspended in 30 µl TE and incubated with 1 U RNase cocktail (Ambion) at 37°C for one hour and then at 4°C over-night. DNA corresponding to the mononucleosomal fraction was purified (QIAEX II gel extraction kit, Qiagen) after separation on a 2% agarose gel and 20 ng of DNA was used for library generation. Library generation and Illumina sequencing was performed by the University of Michigan Sequencing Core.

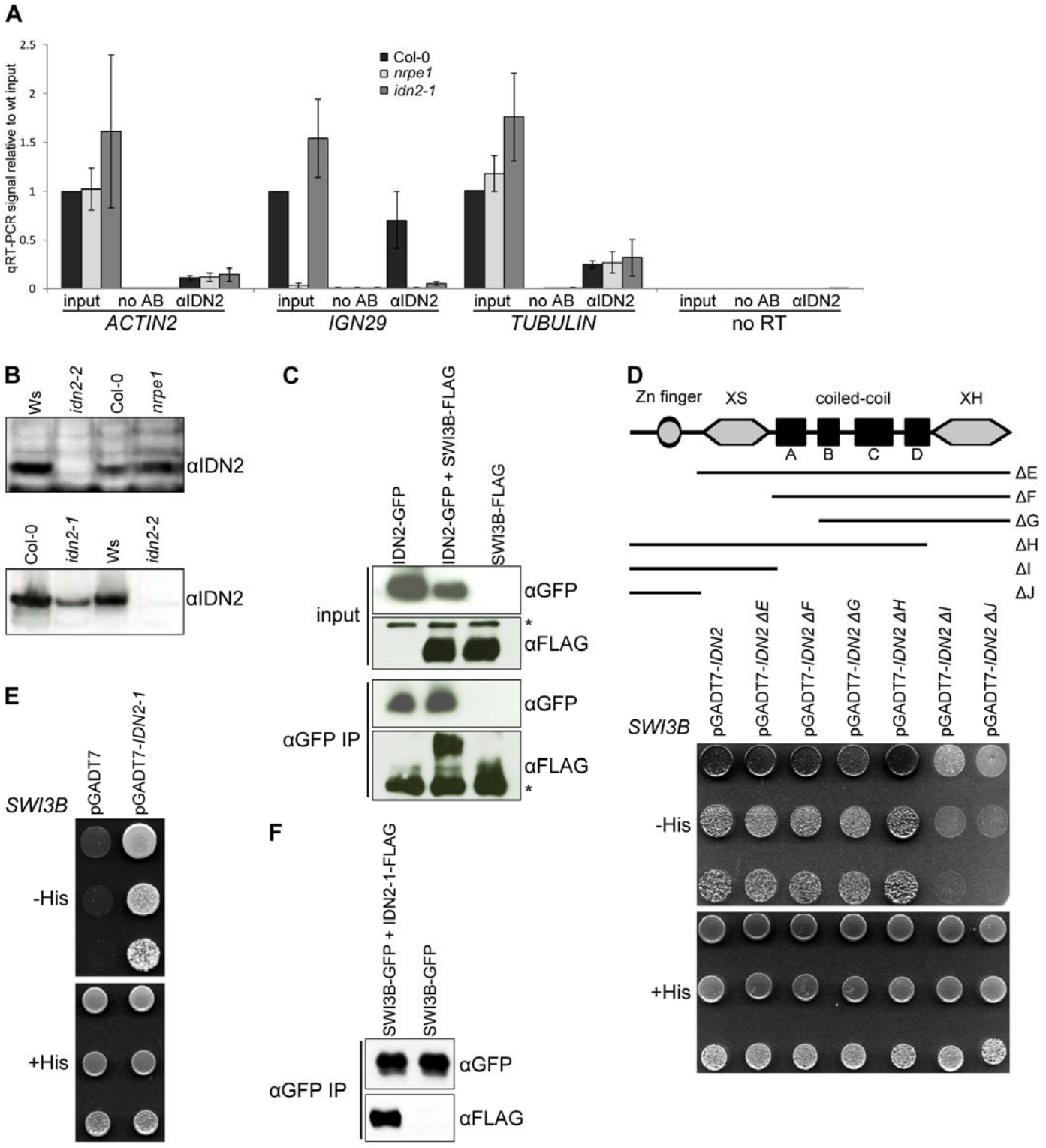

Figure S1. IDN2 interacts with SWI3B, Related to Figure 1

(A) IDN2 interacts with Pol V-produced lncRNA. Input, no antibody and no RT controls as well as RNA IP results shown in Figure 1A were normalized to wild type input. No RT control was performed using *ACTIN2* primers. Bars show averages normalized to wild type inputs and standard deviations from four biological repeats.

(B) IDN2 protein levels. Equal amounts of total protein extracts from *idn2* mutants, *nrpe1* mutant and corresponding wild type controls were assayed using western blot with affinity purified rabbit polyclonal anti-IDN2 antibody.

(C) IDN2 interacts with SWI3B in tobacco. FLAG-tagged SWI3B was coexpressed in tobacco leaves with GFP-tagged IDN2. After immunoprecipitation with anti-GFP antibody the sample was analyzed using western blot with anti-FLAG antibody. Plants expressing only single construct were used as controls. Total protein extracts (inputs) were assayed using western blot to demonstrate comparable protein expression levels. Asterisks indicate non-specific bands. Reciprocal co-immunoprecipitation is shown in Figure 1E.
(D) IDN2 interacts with SWI3B by its coiled-coil domain. Truncated IDN2 was assayed for interactions with SWI3B using yeast two hybrid. A series of three 10x dilutions is shown. Yeast growth on a plate with His is shown as a loading control.
(E) The XS domain within IDN2 is not required for interaction with SWI3B in yeast two hybrid assay. A deletion mutant in the XS domain of IDN2 corresponding to the *idn2-1* mutant (Ausin et al., 2009) was tested for interaction with SWI3B using yeast two hybrid. A series of three 10x dilutions is shown. Yeast growth on a plate with His is shown as a loading control.
(F) The XS domain within IDN2 is not required for interaction with SWI3B in tobacco leaves. A FLAG-tagged deletion mutant in the XS domain of IDN2 corresponding to the *idn2-1* mutant (Ausin et al., 2009) was coexpressed with GFP-tagged SWI3B in tobacco leaves. After immunoprecipitation with anti-GFP antibody the sample was analyzed using western blot with anti-FLAG antibody.

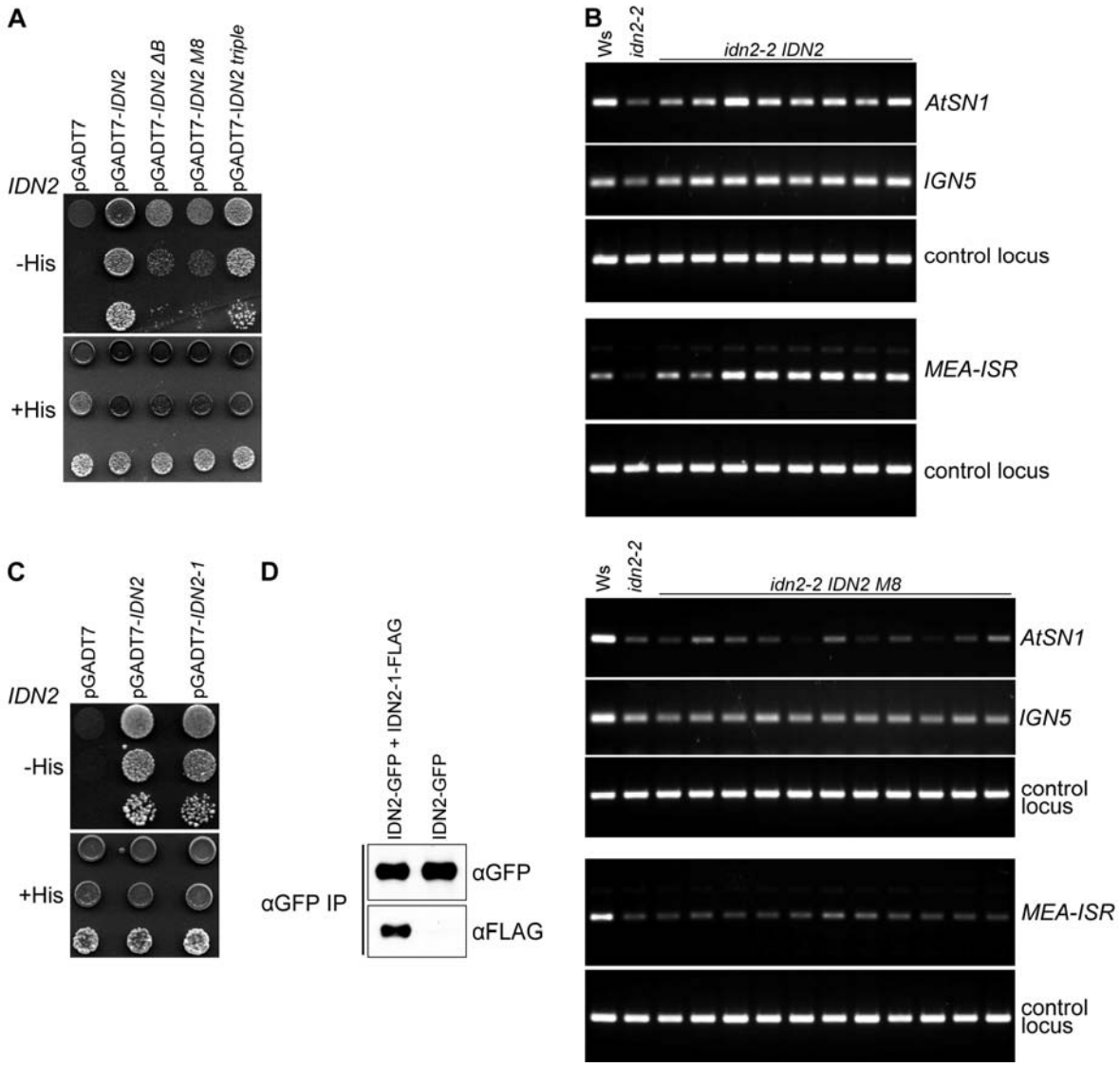

Figure S2. Characterization of IDN2 dimerization domain and its functional significance, Related to Figure 2
(A) Octuple mutations in subdomain B of the coiled-coil region disrupt IDN2 dimerization. Interaction of wild type IDN2, IDN2 with subdomain B deleted, IDN2 with octuple mutations (M8) and IDN2 with triple mutations were assayed for interaction with wild type IDN2 using yeast two-hybrid. A series of three 10x dilutions is shown. Yeast growth on a plate with His is shown as a loading control.
(B) IDN2 dimerization is required for its function – additional independent transgenic lines extending the result shown in Figure 2E. *idn2-2* knock out mutant *Arabidopsis* plants were transformed with wild type *IDN2* or *IDN2 M8*. Obtained transgenic plants were assayed for changes in DNA methylation by digesting with DNA methylation-sensitive restriction endonucleases (*Hae*III for *AtSN1* and *IGN5*, *Sau3*AI for *MEA-ISR*) followed by PCR. Transformation of the *idn2-2* knock out mutant with wild type *IDN2* restored DNA methylation to wild type levels at all tested loci. *IDN2 M8* was unable to restore DNA methylation at any of the tested loci. Sequences with no restriction sites were used as controls (*ACTIN2* for *Hae*III and JA35/JA36 for *Sau3*AI).
(C) The XS domain of IDN2 is not required for dimerization in yeast two hybrid. A mutated IDN2 corresponding to the *idn2-1* mutant was tested for interaction with wild type IDN2 using yeast two hybrid. A series of three 10x dilutions is shown. Yeast growth on a plate with His is shown as a loading control.
(D) The XS domain of IDN2 is not required for dimerization in tobacco leaves. A FLAG-tagged deletion mutant in the XS domain of IDN2 corresponding to the *idn2-1* mutant (Ausin et al., 2009) was coexpressed with GFP-tagged wild type IDN2 in tobacco leaves. After immunoprecipitation with anti-GFP antibody the sample was analyzed using western blot with anti-FLAG antibody.

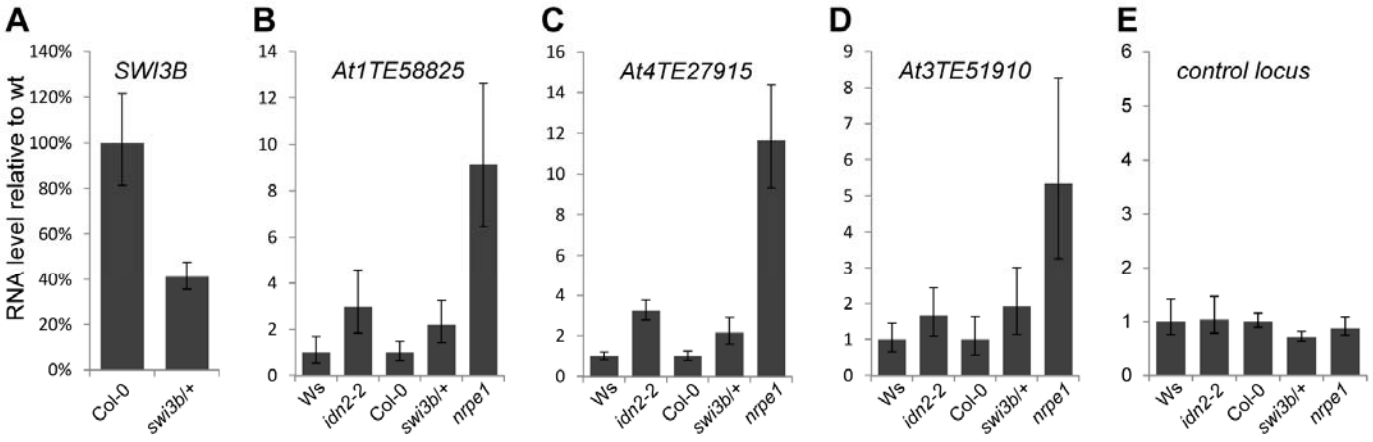

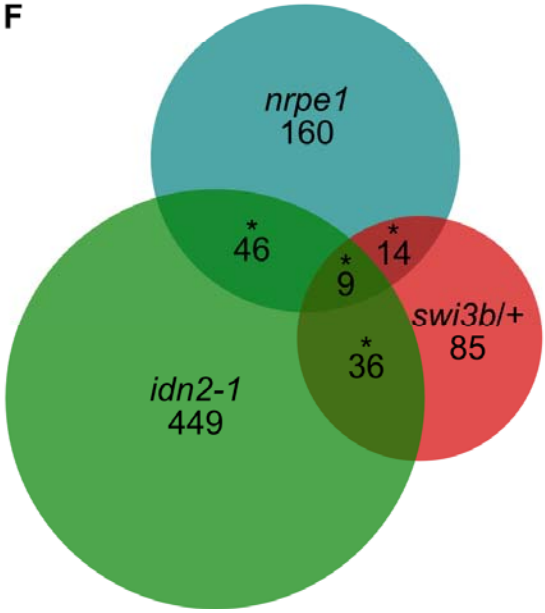

G

		Genes upregulated in:			Genes downregulated in:		
		nrpe1	*idn2*	*swi3b/+*	*nrpe1*	*idn2*	*swi3b/+*
Genes upregulated in:	*nrpe1*		**72** $p < 10^{-298}$	**137** p -> 0		**5** p < 0.9	**2** p < 0.9
	idn2-1	**72** $p < 10^{-298}$		**122** p -> 0	**3** p < 0.9		**3** p < 0.7
	swi3b/+	**137** p -> 0	**122** p -> 0		**2** p < 0.6	**1** p < 0.02	
Genes downregulated in:	*nrpe1*		**3** p < 0.9	**2** p < 0.6		**55** $p < 10^{-127}$	**23** $p < 10^{-87}$
	idn2-1	**5** p < 0.9		**1** p < 0.02	**55** $p < 10^{-127}$		**45** $p < 10^{-140}$
	swi3b/+	**2** p < 0.9	**3** p < 0.7		**23** $p < 10^{-87}$	**45** $p < 10^{-140}$	

Figure S3. SWI3B contributes to RNA-mediated transcriptional silencing, Related to Figure 3

(A) *SWI3B* expression is reduced in the *swi3b*/+ line. RNA accumulation of *SWI3B* was assayed using real time RT-PCR in *swi3b*/+ mutant compared to Col-0 wild type. Graphs show averages and standard deviations from three biological repeats.

(B-E) Silencing targets are derepressed in *swi3b*/+ mutant. RNA accumulation from *At1TE58825*, *At4TE27915* and *At3TE51910* was assayed using real time RT-PCR in *idn2-2* mutant compared to Ws wild type and in *swi3b*/+ and *nrpe1* mutants compared to Col-0 wild type. *UBQ10* was tested as a control (E). Graphs show averages normalized to *ACTIN2* and wild type and standard deviations from three biological repeats.

(F) SWI3B controls the expression levels of a significant subset of Pol V and IDN2 targets. Venn diagram showing genes identified using RNA-seq to be downregulated in *nrpe1, idn2-1* and/or *swi3b*/+ mutants. RNA-seq was performed in three independent biological repeats. * denotes statistically significant enrichment of overlaps (see text and Figure S3G for details).

(G) Overlaps between genes identified by RNA-seq to be upregulated or downregulated in the analyzed mutants. p-values correspond to the observed overlap compared to overlap expected by chance and were obtained using chi-square test.

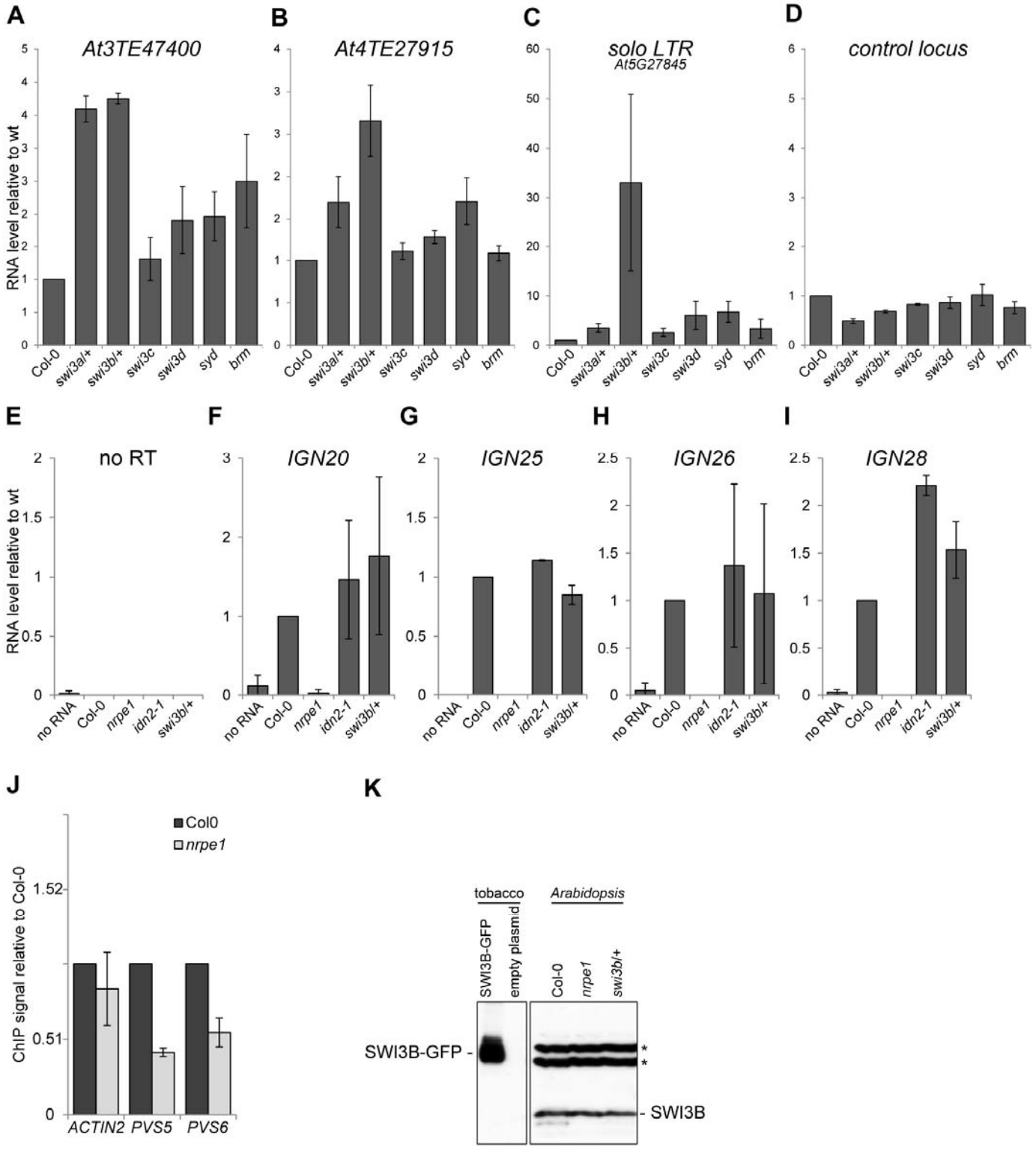

Figure S4. RNA-mediated transcriptional silencing involves the SWI/SNF complex, which works downstream of lncRNA production, Related to Figure 4

(A-D) Silencing targets are derepressed in mutants defective in SWI/SNF subunits. RNA accumulation from *At3TE47400* (A), *At4TE27915* (B) or *At5G27845* (C) was assayed using real time RT-PCR in *swi3a/+, swi3b/+, swi3c, swi3d, syd* and *brm* mutants compared to Col-0 wild type. *ROC3* was tested as a control (D). Graphs show averages normalized to *ACTIN2* and wild type and standard deviations from three biological repeats.

(E-I) IDN2 and SWI3B function downstream of lncRNA production. Pol V-produced lncRNAs *IGN20* (F), *IGN25* (G), *IGN26* (H) and *IGN28* (I) were assayed using real time RT-PCR in *idn2-1* and *swi3b*/+ mutants compared to Col-0 wild type. *nrpe1* mutant was used as a negative control. To check for potential DNA contaminations no RT control was performed on *ACTIN2* (E) and additionally no RNA controls were performed for all primer pairs tested. Graphs show averages normalized to wild type and standard deviations from three biological repeats.
(J) SWI3B binding to chromatin is reduced in the *nrpe1* mutant. ChIP with anti-SWI3B antibody was performed in Col-0 wild type and *nrpe1* mutant. Bars show averages and standard deviations from three biological repeats, normalized to inputs and Col-0. Western blot showing antibody specificity is in (K).
(K) Western blot showing specificity of anti-SWI3B antibody. Total proteins from tobacco leaves expressing epitope-tagged SWI3B and from Col-0, *nrpe1* and *swi3b*/+ *Arabidopsis* plants were assayed using affinity-purified anti-SWI3B antibody. Asterisks indicate non-specific bands detectable only in *Arabidopsis* extracts.

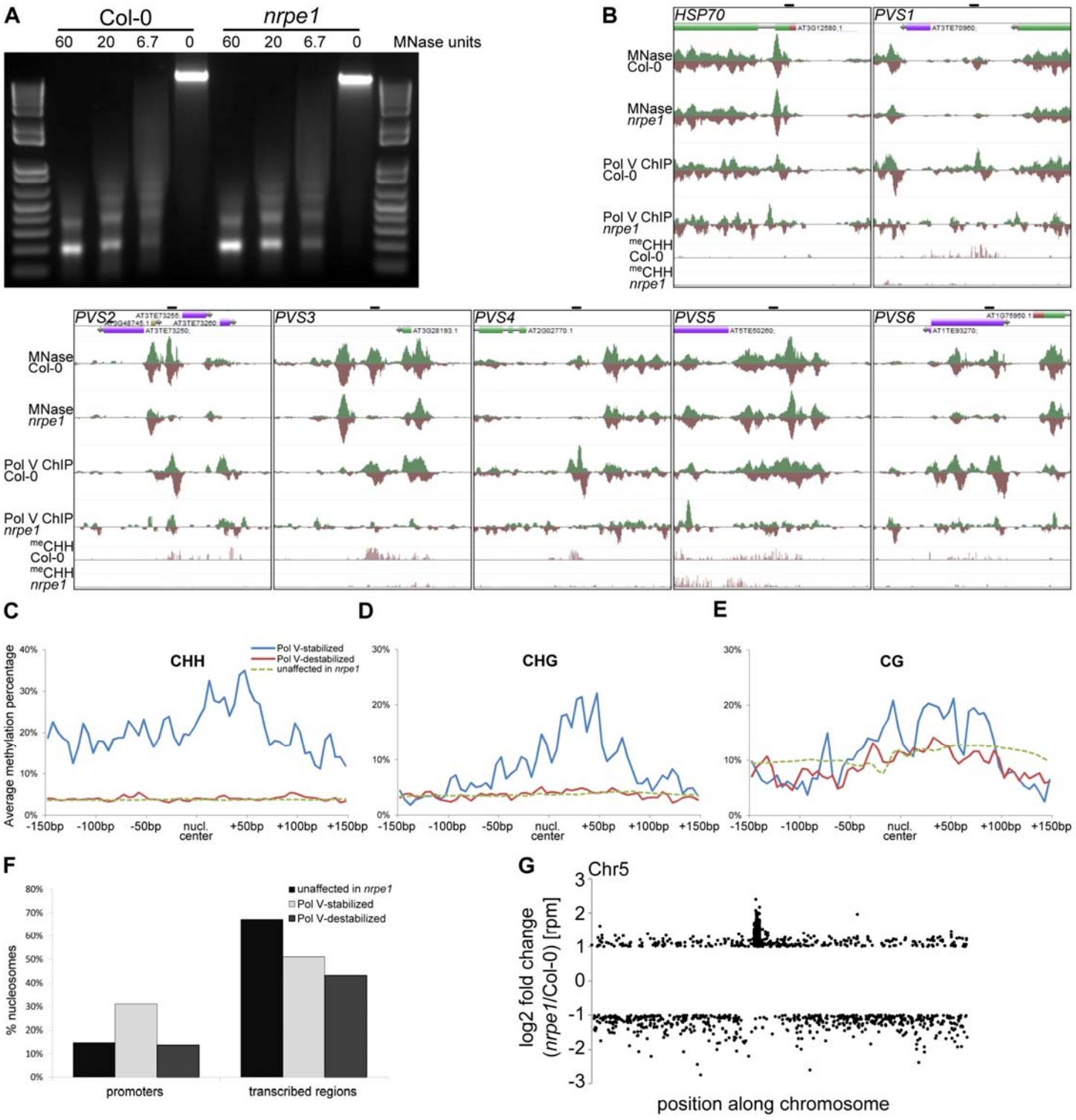

Figure S5. Pol V mediates nucleosome positioning, Related to Figure 5

(A) Micrococcal Nuclease (MNase) digestion of nuclei from Col-0 wild type and *nrpe1* mutant. MNase activity is shown in Kunitz Units. Mononucleosomal DNA was later sequenced using Illumina sequencing.

(B) Genome browser screenshots showing regions of Pol V-stabilized nucleosomes selected for validation (Figure 5A). Shown data include from top: annotation, MNase-seq in Col-0 wild type and *nrpe1* mutant, Pol V ChIP-seq in Col-0 wild type and *nrpe1* mutant (Wierzbicki et al., 2012), CHH methylation in Col-0 wild type and *nrpe1* mutant (Zhong et al., 2012).

(C-E) Nucleosomes stabilized by Pol V are enriched in Pol V-dependent DNA methylation. Profiles of CHH methylation (C), CHG methylation (D) and CG methylation (E) were calculated and plotted on nucleosomes identified using MNase-seq and H3 ChIP-seq with nucleosome center in the middle of each graph. Nucleosomes unaffected in *nrpe1* were tested as controls. Published DNA methylation data were used (Zhong et al., 2012).
(F) Nucleosomes stabilized by Pol V are enriched on gene promoters. Nucleosomes identified using MNase-seq were overlapped with gene promoters and transcribed regions.
(G) Nucleosomes stabilized by Pol V are distributed throughout the chromosomes but nucleosomes destabilized by Pol V are enriched at the centromere. Differential nucleosomes identified using MNase-seq were plotted on the chromosome 5 with the fold value of the change in *nrpe1* mutant compared to Col-0 wild type. Pol V-stabilized nucleosomes have negative and Pol V-destabilized nucleosomes have positive enrichment values.

Table S1. Oligonucleotides used in this study, Related to the Experimental Procedures

Target	Name	Sequence (5'-3')	Application
		Primers for plasmid constructs	
IDN2	proIDN2-F	cacctgttgtagtcgctgtgatac	amplify genomic IDN2
	IDN2-R	agccattccacgcttgcgtttcgc	
IDN2	IDN2-cacc-F	caccatgggaagcactgtgatttta	amplify IDN2 cDNA
	IDN2-R	agccattccacgcttgcgtttcgc	
IDN2	IDN2-pAS2-EcoRI-F	tggaggccgaattcatgggaagcactgtgatt	generate pAS2-IDN2 construct
	IDN2-pAS2-PstI-R	tagcttggctgcagctaagccattccacgcttg	
SWI3B	SWI3b-cacc-F	caccatggccatgaaagctcccga	amplify SWI3B cDNA
	SWI3b-R	acactctattctatcttcagttttcc	
SWI3A	SWI3a-cacc-F	caccatggaagccactgatccaag	amplify SWI3A cDNA
	SWI3a-R	tttcacgtacgtatgatcccaacg	
SWI3D	SWI3d-cacc-F	caccatggaggaaaaacgacgcga	amplify SWI3D cDNA
	SWI3d-R	cgaagaaacattgtctgaacctg	
SWI3C	SWI3C-cacc-F2	caccatgccagcttctgaagatagaagagg	amplify SWI3C cDNA
	SWI3C-R2	taagcctaagccggaccctgagcctgaac	
SWI3B	SWI3B-Pro-CACC-F	caccttaaggcatgcgttgaagcaaaagtt	amplify genomic SWI3B
	SWI3b-R	acactctattctatcttcagttttcc	
Gateway	pEG300F	cgtcacgtcttgcgcactgatttg	generate pZY35S302 vector
	pEG300R	gaaccctgtggttggcatgcac	
		Truncations and site-directed mutagenesis	
IDN2	IDN2-274F	caccatgaaataccttcaacaagatcttgctg	generate IDN2-ΔE deletion
	IDN2-StopR	ctaagccattccacgcttgcgtttcgc	
IDN2	IDN2-721F	caccatgggagaaaacttgaggaagacggg	generate IDN2-ΔF deletion
	IDN2-StopR	ctaagccattccacgcttgcgtttcgc	
IDN2	IDN2-964F	caccatgagtcacattcaaaagatagttg	generate IDN2-ΔG deletion
	IDN2-StopR	ctaagccattccacgcttgcgtttcgc	
IDN2	IDN2-cacc-F	caccatgggaagcactgtgatttta	generate IDN2-ΔH deletion
	IDN2-1521StopR	ctaatttgtgttccattctttcataatgt	
IDN2	IDN2-cacc-F	caccatgggaagcactgtgatttta	generate IDN2-ΔI deletion
	IDN2-759StopR	ctatatagttttcagatcacccgtcttcc	
IDN2	IDN2-cacc-F	caccatgggaagcactgtgatttta	generate IDN2-ΔJ deletion
	IDN2-369StopR	ctaatgatcacaatcttgaatagggtttc	
IDN2	IDN2-del760-897(250-299)F	cttgaggaagacgggtgatctgaaaactataatggaagagaaggagaagaatcagcaaaagc	generate IDN2-ΔA deletion
	IDN2-del760-897(250-299)R	gcttttgctgattcttctccttctcttccattatagttttcagatcacccgtcttcctcaag	
IDN2	IDN2-del964-1059(322-353)F	cgtgagctgaatgctatacaagaaagaacagcaaagcgcgaagtgcacaatggaaccgag	generate IDN2-ΔB deletion
	IDN2-del964-1059(322-353)R	ctcggttccattgtgcacttcgcgctttgctgttctttcttgtatagcattcagctcacg	
IDN2	IDN2-del1153-1320(385-440)F	gcatctaagaatagctctcttgaactagctaagcacatggcatcagatggcgatgctgaag	generate IDN2-ΔC deletion
	IDN2-del1153-1320(385-440)R	cttcagcatcgccatctgatgccatgtgcttagctagttcaagagagctattcttagatgc	
IDN2	IDN2-del1405-1512(469-504)F	cttcaaagatttaggtgagaaggaagcacaaaacacaaatatcggtgttaagagaatgggag	generate IDN2-ΔD deletion
	IDN2-del1405-1512(469-504)R	ctcccattctcttaacaccgatatttgtgttttgtgcttccttctcacctaaatctttgaag	
IDN2	IDN2-I325R/V329G/H332R-F	agaacaatgagtcacagacaaaagataggtgatgatcgtgagaaattgaagagg	generate IDN2 triple mutant
	IDN2-I325R/V329G/H332R-R	cctcttcaatttctcacgatcatcacctatcttttgtctgtgactcattgttct	
IDN2	IDN2-MM5on3-F	gatgatcgtgagaaattggggaggctgagggagtcagaggggaagaaacgcgaaatcaaaggtaatgagttggcaaagc	generate IDN2 octuple mutant (M8)
	IDN2-MM5on3-R	gctttgccaactcattaccttgatttcgcgtttcttcccctctgactccctcagcctcccca atttctcacgatcatc	

RNA detection

SWI3B	Swi3b-qRT-F2	cggcgaagttgcgttagttaaaca	real time RT-PCR
	Swi3b-qRT-R2	cctccagacgtagtttcggaaaga	
ACTIN2	Actin2-A118	gagagattcagatgcccagaagtc	real time RT-PCR RNA IP-qPCR
	Actin2-A119	tggattccagcagcttcca	
soloLTR (At5TE35950)	soloLTR-F4	tcatgttaaaaccgattgcaccattt	real time RT-PCR
	soloLTR-R4	caaaaattaggatcttgtttgccagcta	
soloLTR (At5G27845)	IG-up-F8	cggaatggggaaatttcaaggacgc	real time RT-PCR
	IG-up-R8	cagtgacgctgtcaccctcgaa	
At1TE51360	LTRCO1-F3	gccgaatggctcattaagtacctg	real time RT-PCR
	LTRCO1-R3	aagtgggtattcgtgcgaaaaaga	
At3TE51910	LTRCO3-F2	ataaccttcccacgctgcattaga	real time RT-PCR
	LTRCO3-R2	tgtgagcctgaaggagatgttgac	
At2TE78930	78930F1	ttgattaatgatcgcgaaaaagta	real time RT-PCR
	78930FR1	taatgagtgttgatcggaaagaga	
At1TE58825	58825F1	acttacgcatctcattgtgttgtt	real time RT-PCR
	58825R1	atcctctcttccttgtcatgattc	
At4TE27915	27915F1	attcaatcgctccggtaaaatcct	real time RT-PCR
	27915R1	agatcgtggtctcgtctgttttcc	
At3TE47400	IG12F1	cgaagcttcccacaaaatatcgtc	real time RT-PCR
	IG12R1	gagggaaggagaaggagcagaatc	
TUBULIN8	JR147	gcttactaatcaaagatgcgaga	real time RT-PCR
	JR148	cttggtatcttcccgtcgaa	
UBQ10	GB473_UBQ10s_fw	ccatcacccttgaagtggaa	real time RT-PCR
	GB474_UBQ10s_rv	gatcttggccttgacgttgt	
ROC3	GB469_ROC3s_fw	aaggttggatctgactctggaa	real time RT-PCR
	GB470_ROC3s_rv	tctgaccacaatcagcaatga	
25S rRNA	JR41	tgttcacccaccaatagggaa	RNA IP-qPCR
	JR42	tcagtagggtaaaactaacctgtctc	
IGN5	GB268_IGN5-A	acatgaagaaagcccaaacc	real time RT-PCR
	GB269_IGN5-A	gccgaataacagcaagtcct	
IGN20	GB280_IGN20	aagaaccggaccaatacgg	real time RT-PCR
	GB281_IGN20	ccaccgcctctattgaaatg	
IGN22	GB282_IGN22	tggtccataggttcggaattt	real time RT-PCR
	GB283_IGN22	ggcatggtttgatatcaggag	
IGN25	GB288_IGN25	aaacccacctctttaggtcca	real time RT-PCR
	GB289_IGN25	ggcttggagagtccaacaat	
IGN26	GB290_IGN26	cgttgttccgcctaattctg	real time RT-PCR
	GB291_IGN26	gccaggaaaccctaacttcc	
IGN27	JA13	ggatttaacgacatttttcccttca	real time RT-PCR
	JA14	ggcttagggcccgtaactaataaat	
IGN28	JA17	atgtggatggatttgttaaccctct	real time RT-PCR
	JA18	gaagaacgaagaacaatgtgttgac	
IGN29	JA227	cgtttgtttatgtagggcgaaag	real time RT-PCR RNA IP-qPCR
	JA228	taaaacttttcccgccaacca	
IGN30	GB402_PV-3	gtgtgatgatgtatcatttatatggag	real time RT-PCR RNA IP-qPCR
	GB403_PV-3	atatatgaaaattggcctacactctc	
IGN31	GB416	caatctggcacacacgaaac	real time RT-PCR RNA IP-qPCR
	GB417	caggttggatctgttgacga	
IGN32	GB424	ccgaaaccacagcatgtaat	real time RT-PCR RNA IP-qPCR
	GB425	tgaaattttcgcatcacaaca	
IGN33	GB418	tctcttaggttccaccggatt	real time RT-PCR RNA IP-qPCR
	GB419	cgggtttcattcgtcttcat	

DNA methylation assays

soloLTR (At5TE35950)	soloLTR-C-F(A211)(AluI)	ataaaactcgaaacaagagttttcttattgctttc	Chop qPCR, AluI
	soloLTR-C-R(A212)(AluI)	taatggtattattttgatcagtgttataaaccgga	
siR02	siR02chop-qPCR-F(AluI)	atagtgcagttccgaaacagtaaaccat	Chop qPCR, AluI
	siR02chop-qPCR-R(AluI)	tcaaagtgaaagtggttcttgggtttat	
At2TE78930	78930M1-F(AvaII)	atcaatacaaggtccatcaacaaa	Chop qPCR, AvaII
	78930M1-R(AvaII)	gggattgagggtttgagtttaggg	
JA35/JA36	JA35	ggcgaccttctcgagtttcc	Chop qPCR
	JA36	caagaaccccaccccataca	
IGN6	IGN6-A30(AluI)	gggacatctattgggtttaggctggatg	Chop qPCR, AluI, (Wierzbicki et al., 2008)
	IGN6-A31(AluI)	tttgtaattctcagttcgggtatctgcttg	
IGN22	IGN22-A413(AvaII)	caaaaatattcacccgctacaaacaaaaa	Chop-qPCR, AvaII, (Rowley et al., 2011)
	IGN22-A414(AvaII)	tcttccatttgtggggcatggt	
At3TE51910	51910M-F1(NlaIII)	tattacattgtcccccgctatca	Chop qPCR, NlaIII
	51910M-R1(NlaIII)	ggtggaagcataaaggattaggg	
AtSN1	AtSN1-A32(HaeIII)	accaacgtgctgttggcccagtggtaaatc	Chop PCR, HaeIII, (Herr et al., 2005)
	AtSN1-A33(HaeIII)	aaaataagtggtggttgtacaagc	
IGN5	IGN5-A28(HaeIII)	tcccgagaagagtagaacaaatgctaaaa	Chop PCR, HaeIII, (Wierzbicki et al., 2008)
	IGN5-A29(HaeIII)	ctgaggtattccatagcccctgatcc	
MEA-ISR	MEA-ISR-F(Sau3AI)	aaaaagctctttaaaatccgaaagtaac	Chop PCR, Sau3AI
	MEA-ISR-R(Sau3AI)	acattgtgaaatctaaccggattttgga	
ACTIN2	Actin2g-qPCR-F;	tttatttgctggatctcgatcttgtttt	Chop qPCR, non cutting control for AluI, AvaII, NlaIII
	Actin2g-qPCR-R;	aaaccaaaagatttagtggaggttcaca	
ACTIN2	Actin2g-qPCR-F2;	agtgtcgtacgttgaacagaaagc	Chop qPCR, non cutting control for Sau3AI
	Actin2g-qPCR-R2;	gagctgcaaacacacaaaaagagt	
ACTIN2	ACTIN2-A65	cgagcaggagatggaaacctcaaa	Chop PCR, non cutting control for HaeIII, (Wierzbicki et al., 2008)
	ACTIN2-A66	aagaatggaaccaccgatccagaca	

Nucleosome validation

PVS1	JR339	gaaaattagagagtgaaacgagagca	ChIP-qPCR
	JR340	tttattggcctgccctatttg	
PVS2	JR377	ccttcaaggggtgtgaaaaga	ChIP-qPCR
	JR378	tctccttcttcgctgccaaa	
PVS3	JR379	cccacaaaaatggttttccatc	ChIP-qPCR
	JR380	caagcccaacatctcggaaa	
PVS4	JR381	cccattggtccatttggtgt	ChIP-qPCR
	JR382	gggcctgtagtggccttgta	
PVS5	JR555	agttggatggagtccacgac	ChIP-qPCR
	JR556	cgctctctgcaattttgctt	
PVS6	JR575	aaggagaagagacgagttgatga	ChIP-qPCR
	JR576	tgcctcttgcgaaaacaaca	
ACTIN2	Actin2-A118	gagagattcagatgcccagaagtc	ChIP-qPCR (Wierzbicki et al., 2008)
	Actin2-A119	tggattccagcagcttcca	
HSP70	A512	ctcttcctcacacaatcataaaca	ChIP-qPCR (Kumar and Wigge, 2010)
	A513	cagaattgttcgccggaaag	

SUPPLEMENTAL REFERENCES

Ausin, I., Mockler, T.C., Chory, J., and Jacobsen, S.E. (2009). IDN1 and IDN2 are required for de novo DNA methylation in Arabidopsis thaliana. Nat. Struct. Mol. Biol. *16*, 1325–1327.

Clough, S.J., and Bent, A.F. (1998). Floral dip: a simplified method for Agrobacterium-mediated transformation of Arabidopsis thaliana. Plant J. *16*, 735–743.

Curtis, M.D., and Grossniklaus, U. (2003). A gateway cloning vector set for high-throughput functional analysis of genes in planta. Plant Physiol. *133*, 462–469.

Earley, K.W., Haag, J.R., Pontes, O., Opper, K., Juehne, T., Song, K., and Pikaard, C.S. (2006). Gateway-compatible vectors for plant functional genomics and proteomics. Plant J. *45*, 616–629.

Fankhauser, C., Yeh, K.C., Lagarias, J.C., Zhang, H., Elich, T.D., and Chory, J. (1999). PKS1, a substrate phosphorylated by phytochrome that modulates light signaling in Arabidopsis. Science *284*, 1539–1541.

Herr, A.J., Jensen, M.B., Dalmay, T., and Baulcombe, D.C. (2005). RNA polymerase IV directs silencing of endogenous DNA. Science *308*, 118–120.

Kim, J., Harter, K., and Theologis, A. (1997). Protein-protein interactions among the Aux/IAA proteins. Proc. Natl. Acad. Sci. U.S.A. *94*, 11786–11791.

Kumar, S.V., and Wigge, P.A. (2010). H2A.Z-containing nucleosomes mediate the thermosensory response in Arabidopsis. Cell *140*, 136–147.

Lawit, S.J., O'Grady, K., Gurley, W.B., and Czarnecka-Verner, E. (2007). Yeast two-hybrid map of Arabidopsis TFIID. Plant Mol. Biol. *64*, 73–87.

Rowley, M.J., Avrutsky, M.I., Sifuentes, C.J., Pereira, L., and Wierzbicki, A.T. (2011). Independent chromatin binding of ARGONAUTE4 and SPT5L/KTF1 mediates transcriptional gene silencing. PLoS Genet. *7*, e1002120.

Shin, H., Liu, T., Manrai, A.K., and Liu, X.S. (2009). CEAS: cis-regulatory element annotation system. Bioinformatics *25*, 2605–2606.

Voinnet, O., Rivas, S., Mestre, P., and Baulcombe, D. (2003). An enhanced transient expression system in plants based on suppression of gene silencing by the p19 protein of tomato bushy stunt virus. Plant J. *33*, 949–956.

Weiner, A., Hughes, A., Yassour, M., Rando, O.J., and Friedman, N. (2010). High-resolution nucleosome mapping reveals transcription-dependent promoter packaging. Genome Res. *20*, 90–100.

Wierzbicki, A.T., Cocklin, R., Mayampurath, A., Lister, R., Rowley, M.J., Gregory, B.D., Ecker, J.R., Tang, H., and Pikaard, C.S. (2012). Spatial and functional relationships among Pol V-associated loci, Pol IV-dependent siRNAs, and cytosine methylation in the Arabidopsis epigenome. Genes Dev. *26*, 1825–1836.

Wierzbicki, A.T., Haag, J.R., and Pikaard, C.S. (2008). Noncoding transcription by RNA polymerase Pol IVb/Pol V mediates transcriptional silencing of overlapping and adjacent genes. Cell *135*, 635–648.

Zhong, X., Hale, C.J., Law, J.A., Johnson, L.M., Feng, S., Tu, A., and Jacobsen, S.E. (2012). DDR complex facilitates global association of RNA polymerase V to promoters and evolutionarily young transposons. Nat. Struct. Mol. Biol. *19*, 870–875.